Supplementary Information

Probing Photoreactions of Individual Suspended Carbonaceous Aerosols by Multi-Wavelength OT-SERS

Hang Zhong, [a] Jun Chen, *[a] Yi Hu, [a] Jun Chen, [a] Tao Shao, [a] and Junsheng Liao, *[b]

Affiliations:

[a] Science and Technology on Surface Physics and Chemistry Laboratory, Jiangyou 621908, China

[b] Institute of Materials, China Academy of Engineering Physics, Mianyang 621907, China

Corresponding Author

Jun Chen, E-mail: junchen76@163.com

Junsheng Liao, E-mail: jshliao64@163.com

Table S1

Plasmon resonance peak positions of AgNPs at different growth generations

generation	SPR dipolar (nm)	SPR quadrupolar (nm)
1	407	
2	413	
3	419	
4	423	
5	428	
6	431	
7	437	
8	439	
9	444	
10	447	
11	451	
12	455	
13	458	
14	464	
15	473	404
16	482	407
17	487	412
18	496	417
19	506	421
20	519	423
21	532	426
22	547	431
23	563	434
24	576	437
25	599	444
26	622	451
27	641	456

Table S2

The assignments of Raman peaks of 4-MBA[1-4]

4-MBA	
Raman shift (cm^{-1})	Assignment
1078	ν(CS) + ν(CC)
1141	δ(CH)
1182	δ(CH)
1418	$\nu_s(COO^-)$
1480	ν(CC) + δ(CH)
1584	ν(CC)

1. C. J. Orendorff, A. Gole, T. K. Sau and C. J. Murphy, Anal. Chem., 2005, 77, 3261.
2. H. Yeasmin, M. Akteruzzaman, M. Motiur Rahaman Mazumder, S. Y. Alfaifi, R. H. Althomali and M. M. Rahman, J. Photoch. Photobio. A, 2024, 448.
3. T. Shao, J. Xu, H. Zhong, Y. Hu and J. Chen, Talanta, 2024, 274, 126008.
4. S. Zhu, C. Fan, J. Wang, J. He and E. Liang, Appl. Phys. A, 2014, 117, 1075.

Table S3

The optimized geometric structures and optimized coordinates of possible reaction products from DFT calculations.

Optimized geometric structures	Symbol	X	Y	Z
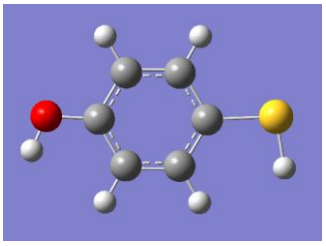 4-mercaptophenol	C	-1.8418	0.013706	0.000001
	C	-1.13337	1.215551	-0.000004
	C	0.255585	1.204921	-0.000008
	C	0.962996	-0.002811	-0.000003
	C	0.248124	-1.201371	0.000007
	C	-1.14562	-1.194031	0.000005
	S	2.752025	0.072117	0.000013
	O	-3.2105	0.085132	0.000004
	H	-1.68034	2.150524	-0.00001
	H	0.791542	2.147487	-0.000016
	H	0.768097	-2.152574	0.000017
	H	-1.6861	-2.136142	0.000011
	H	2.966627	-1.257799	-0.000189
	H	-3.58378	-0.802215	-0.000036
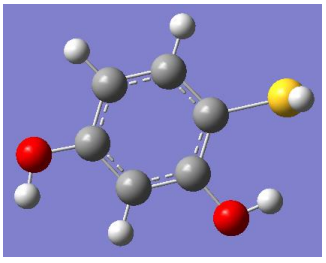 2,4-dihydroxybenzenethiol	C	-1.16531	1.0448	-0.00437
	C	0.225328	0.922212	0.002876
	C	0.82006	-0.35147	-0.00473
	C	-0.00112	-1.48294	0.013433
	C	-1.38312	-1.37141	0.005352
	C	-1.96083	-0.09735	-0.00503
	S	2.61017	-0.48358	0.073639
	O	-3.32446	-0.03154	-0.01163
	O	0.955221	2.063861	0.004266
	H	-1.60052	2.038445	-0.00482
	H	0.459462	-2.4634	0.0312
	H	-2.02113	-2.24549	0.014095
	H	2.859529	-0.53724	-1.25587
	H	-3.60939	0.888452	-0.01055
	H	1.893116	1.814891	0.06146
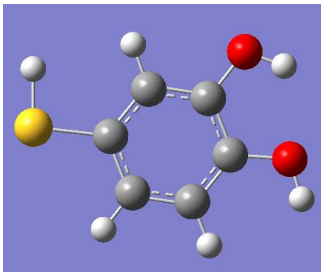 3,4-dihydroxybenzenethiol	C	0.691792	-1.591952	0.000005
	C	-0.687118	-1.383139	0.000015
	C	-1.193658	-0.081768	0.000008
	C	-0.314735	1.004849	-0.000017
	C	1.058936	0.792688	-0.000003
	C	1.564655	-0.513695	0.000002
	S	-2.971736	0.122157	-0.000033
	O	2.940675	-0.611642	0.000002
	O	1.900061	1.864386	-0.000006
	H	1.083843	-2.60458	0.000011
	H	-1.356833	-2.234498	0.000035
	H	-0.67081	2.027944	-0.000041
	H	-2.978071	1.469033	0.000497
	H	3.2153	-1.533598	0.000026
	H	2.809221	1.537338	-0.000025

Table S3 (continued)

The optimized geometric structures and optimized coordinates of possible reaction products from DFT calculations.

Optimized geometric structures	Symbol	X	Y	Z
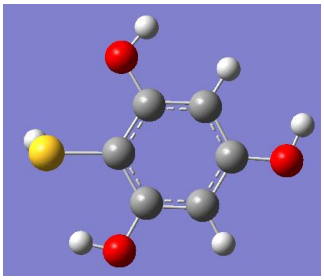 2,4,6-trihydroxybenzenethiol	C	2.018881	-0.07037	0.00254
	C	1.302635	-1.26053	-0.00345
	C	-0.08943	-1.20989	-0.00838
	C	-0.77671	0.021428	-0.00431
	C	-0.02627	1.204954	0.000088
	C	1.368107	1.167157	-0.00034
	S	-2.56245	0.02391	0.093964
	O	3.380728	-0.16618	0.005775
	O	-0.75747	-2.38565	-0.02038
	O	-0.70841	2.384261	-0.0142
	H	1.814066	-2.21317	-0.00594
	H	1.939019	2.091386	-0.00759
	H	-2.83268	0.317777	-1.19893
	H	3.773384	0.712687	0.015746
	H	-1.70966	-2.18576	-0.02285
	H	-0.0871	3.118569	0.029668
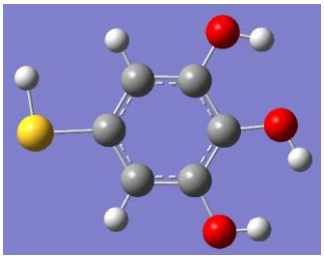 3,4,5-trihydroxybenzenethiol	C	0.757293	-1.209746	0.000003
	C	-0.636736	-1.20017	0.000025
	C	-1.327758	0.009941	0.000014
	C	-0.629965	1.219195	-0.000027
	C	0.759422	1.202692	-0.00001
	C	1.464303	-0.007153	-0.000004
	S	-3.113996	-0.064155	-0.000034
	O	2.845558	0.131767	0.000005
	O	1.435749	2.384887	-0.000011
	O	1.356498	-2.448117	-0.000005
	H	-1.153106	-2.151756	0.000057
	H	-1.132388	2.177749	-0.00006
	H	-3.326438	1.265897	0.000553
	H	3.314936	-0.705252	0.00018
	H	2.383628	2.198327	-0.000008
	H	2.315506	-2.395327	-0.000092
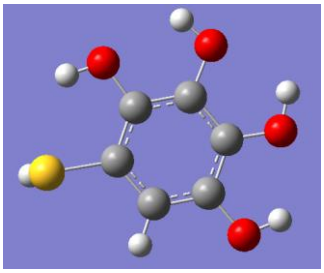 2,3,4,5-tetrahydroxybenzenethiol	C	0.703412	1.109135	-0.00383
	C	-0.67089	0.866855	0.001211
	C	-1.13816	-0.4497	-0.006202
	C	-0.2316	-1.5164	0.009341
	C	1.134655	-1.27102	-0.000668
	C	1.600512	0.048993	-0.005606
	S	-2.91255	-0.72354	0.076891
	O	2.954402	0.24626	-0.008306
	O	2.016268	-2.31459	0.00311
	O	1.225445	2.376442	-0.003102
	O	-1.47165	1.977181	-0.000086
	H	-0.58542	-2.53858	0.026082
	H	-3.15042	-0.82203	-1.251731
	H	3.135863	1.194961	0.001796
	H	2.914012	-1.95875	0.01048
	H	0.497228	3.011005	0.016313
	H	-2.3938	1.68054	0.068403

Table S3 (continued)

The optimized geometric structures and optimized coordinates of possible reaction products from DFT calculations.

Optimized geometric structures	Symbol	X	Y	Z
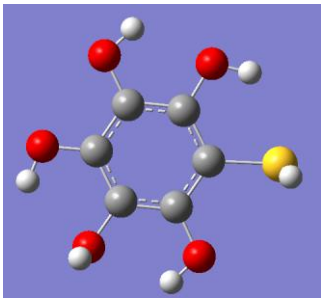 pentahydroxybenzenethiol	C	-1.69139	0.153482	-0.0111
	C	-0.90171	1.303633	0.007957
	C	0.487714	1.16113	0.027699
	C	1.109485	-0.09813	0.015323
	C	0.305814	-1.24418	-0.00181
	C	-1.07962	-1.10408	0.02622
	S	2.891726	-0.17612	-0.10357
	O	1.193461	2.328294	0.04848
	O	-1.49329	2.532911	-0.00332
	O	-3.04278	0.270812	-0.04729
	O	-1.88665	-2.24738	-0.02673
	O	0.876151	-2.48031	-0.01675
	H	3.161314	-0.49645	1.183065
	H	2.140289	2.107355	0.040645
	H	-0.79268	3.197864	-0.00613
	H	-3.40796	-0.60391	-0.23802
	H	-2.10498	-2.53135	0.870413
	H	0.179592	-3.12131	-0.21372

Table S4

The vibrational frequencies of possible reaction products from DFT calculations.

Reaction products	Vibrational frequencies (cm^{-1})	Reaction products	Vibrational frequencies (cm^{-1})
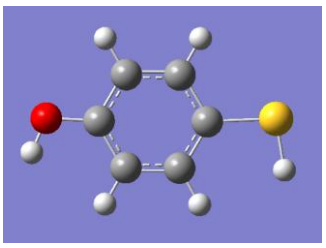 4-mercaptophenol	1076 1150 1163 1240 1281 1316 1480 1576 1595	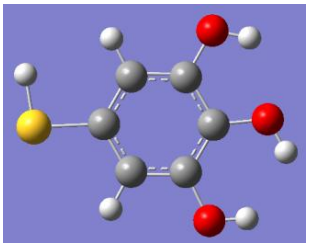 3,4,5-trihydroxybenzenethiol	1065 1125 1150 1165 1228 1268 1334 1444 1481 1588 1609
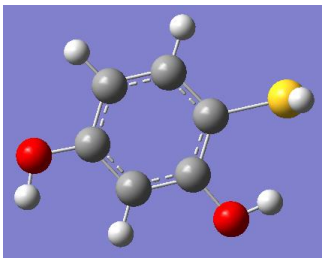 2,4-dihydroxybenzenethiol	1031 1108 1151 1163 1198 1250 1301 1338 1439 1472 1578 1597	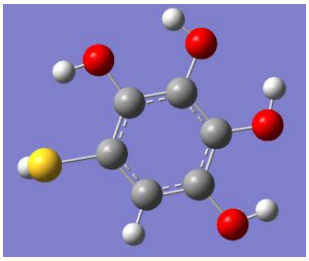 2,3,4,5-tetrahydroxybenzenethiol	1050 1143 1161 1208 1229 1253 1282 1335 1375 1466 1496 1605 1623
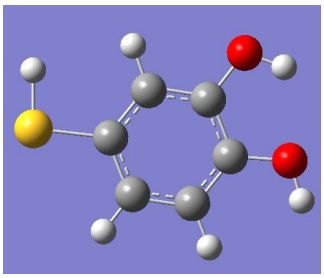 3,4-dihydroxybenzenethiol	1062 1136 1173 1221 1261 1302 1320 1437 1486 1588 1601	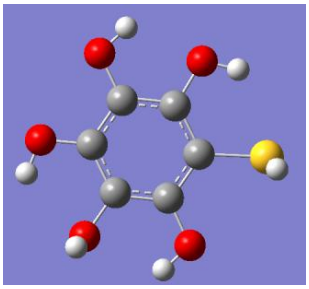 pentahydroxybenzenethiol	1061 1096 1167 1190 1255 1270 1304 1353 1386 1492 1602 1620
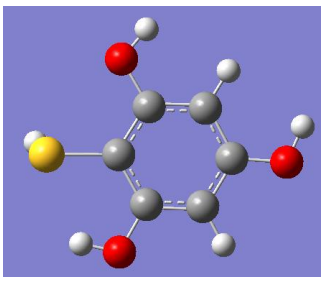 2,4,6-trihydroxybenzenethiol	1025 1052 1127 1157 1190 1205 1344 1352 1583 1607		

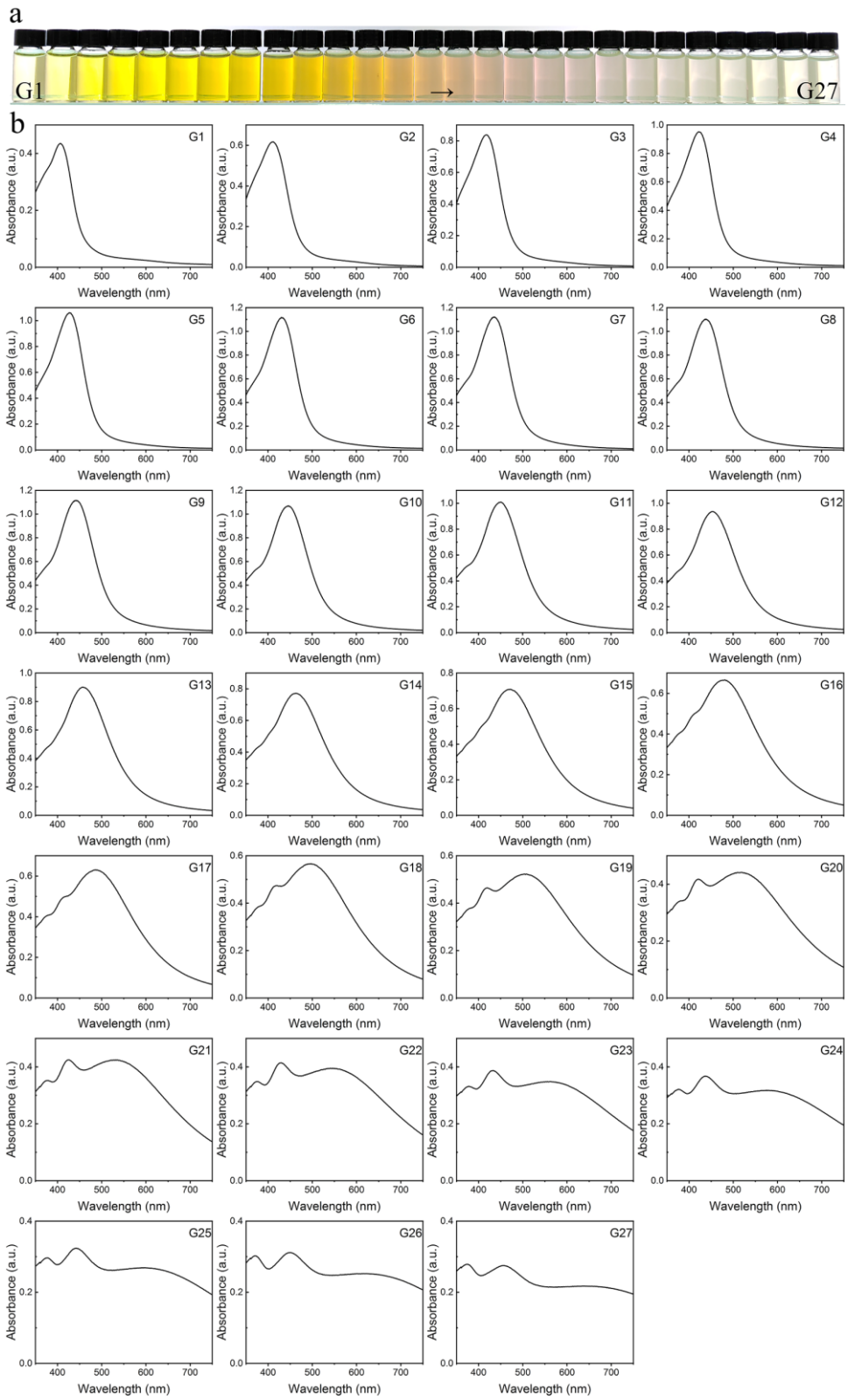

Fig. S1. (a) Photographs and (b) UV-Vis absorption spectra of the different generations of AgNPs solutions.

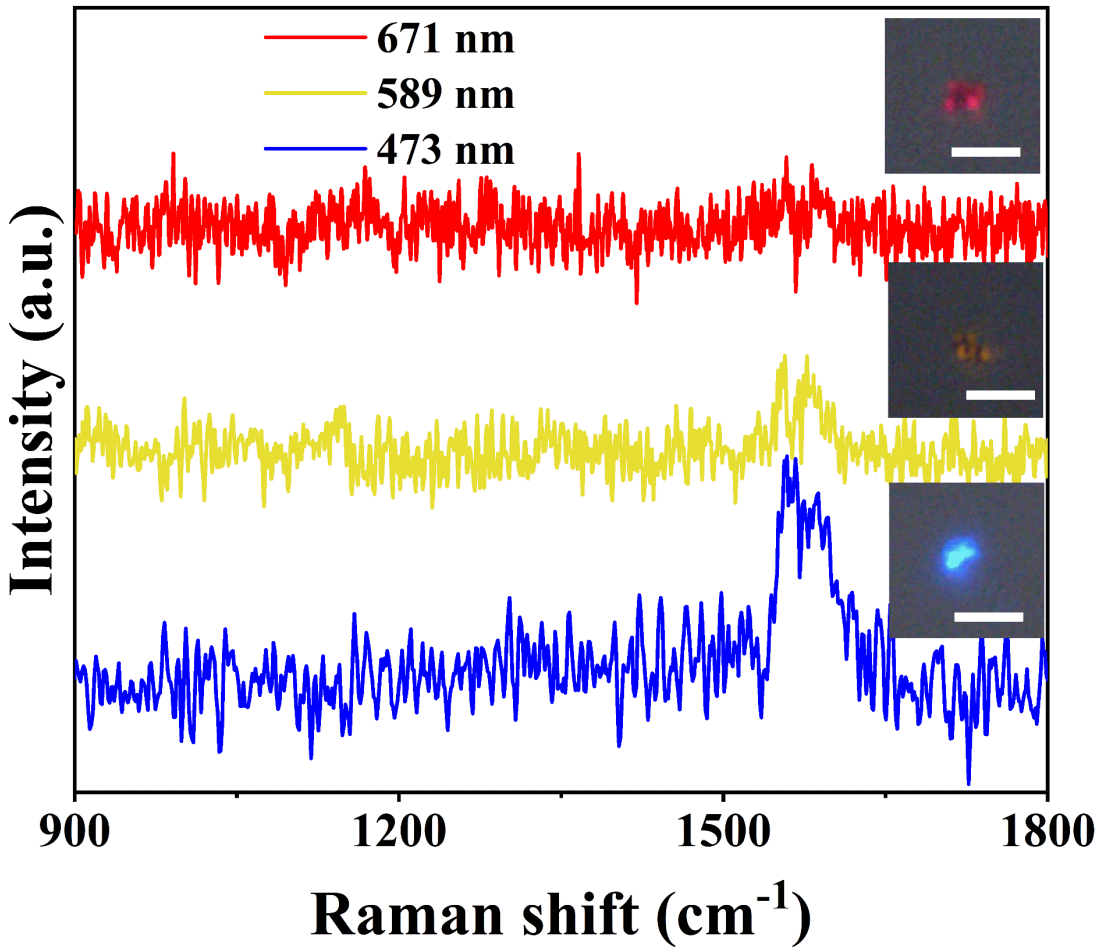

Fig. S2. OT-Raman and optical images of 4-MB/C particles under trapping and excitation by lasers with wavelengths of 473 nm, 589 nm, and 671 nm. Scale bar: 10 μm.

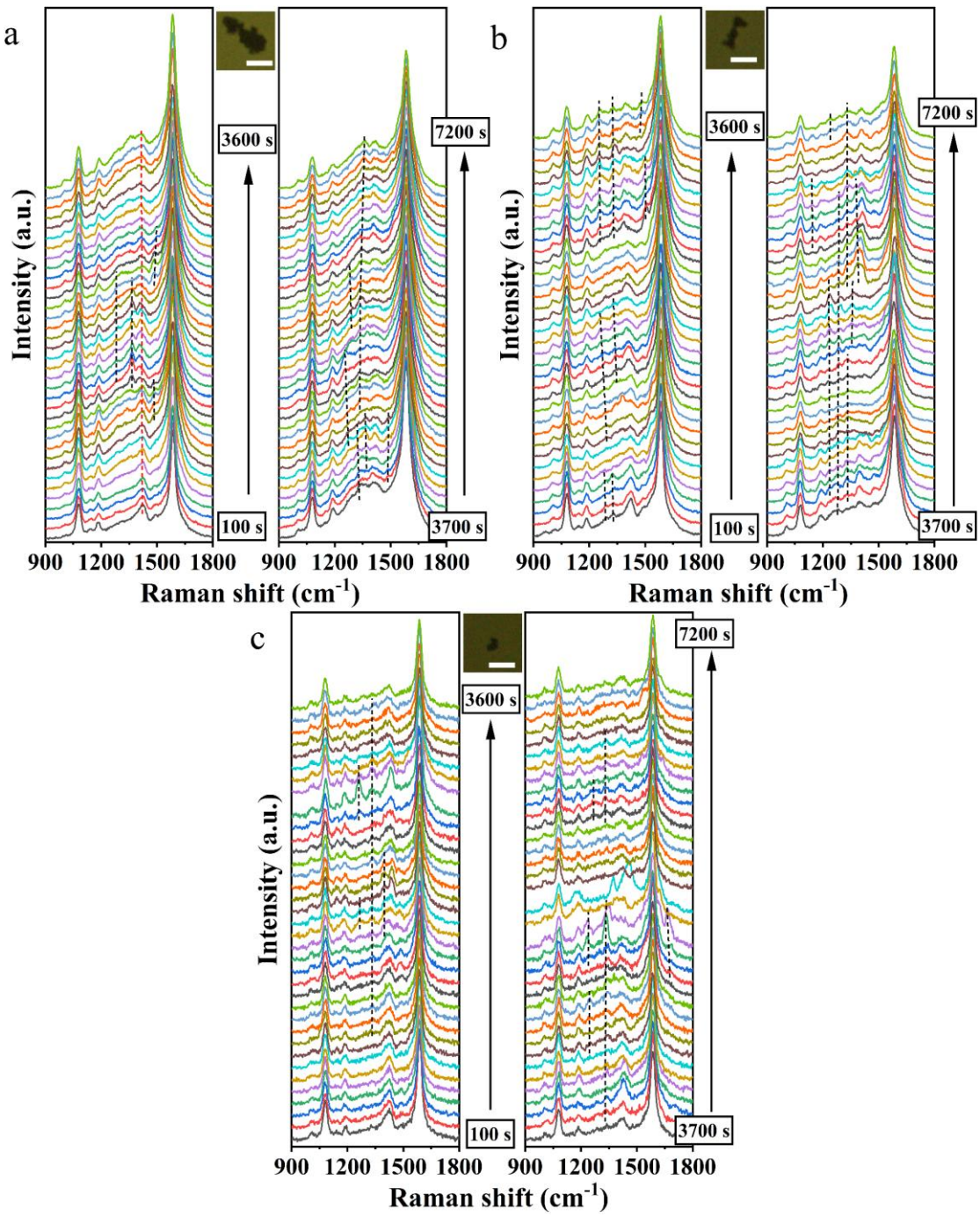

Fig. S3. (a-c) Temporal OT-SERS spectra and optical image of three 4-MBA/AgNPs/C particles under 473 nm laser irradiation. Scale bar: 10 μm.

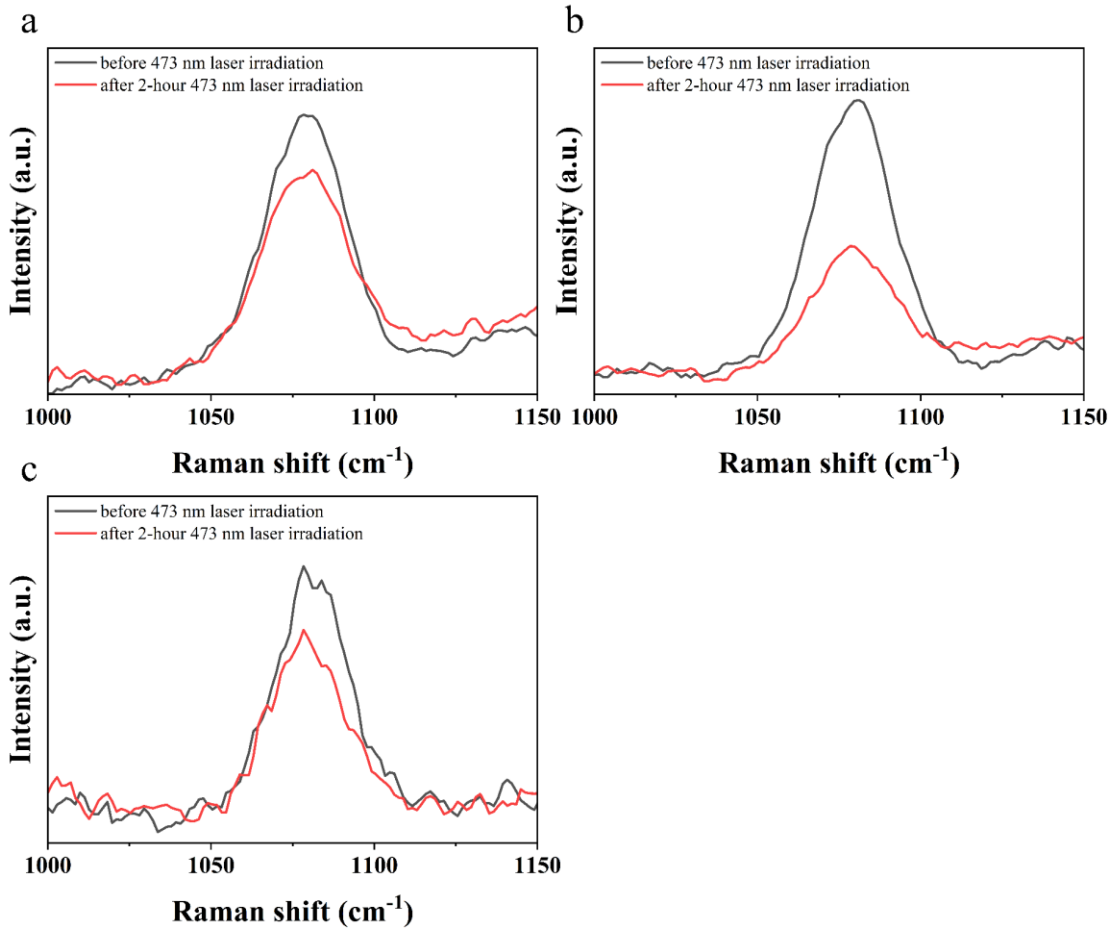

Fig. S4. (a-c) Raman peak at 1078 cm^{-1} of 4-MBA/AgNPs/C particle (from the corresponding panels of Fig. S3.a-S3.c) before and after 473 nm laser irradiation for 2 h.

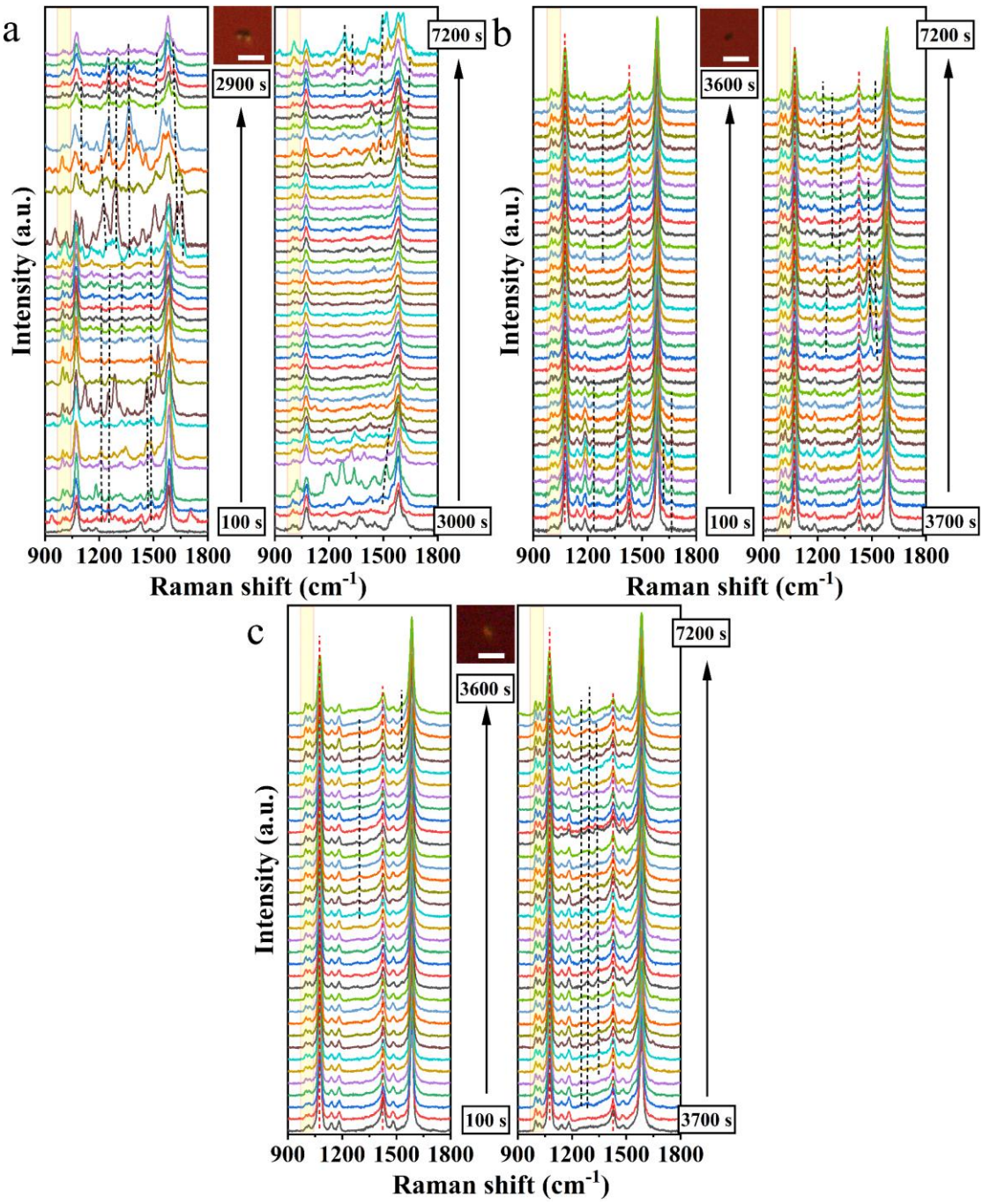

Fig. S5. (a-c) Temporal OT-SERS spectra and optical image of three 4-MBA/AgNPs/C particles under 589 nm laser irradiation. Scale bar: 10 μm.

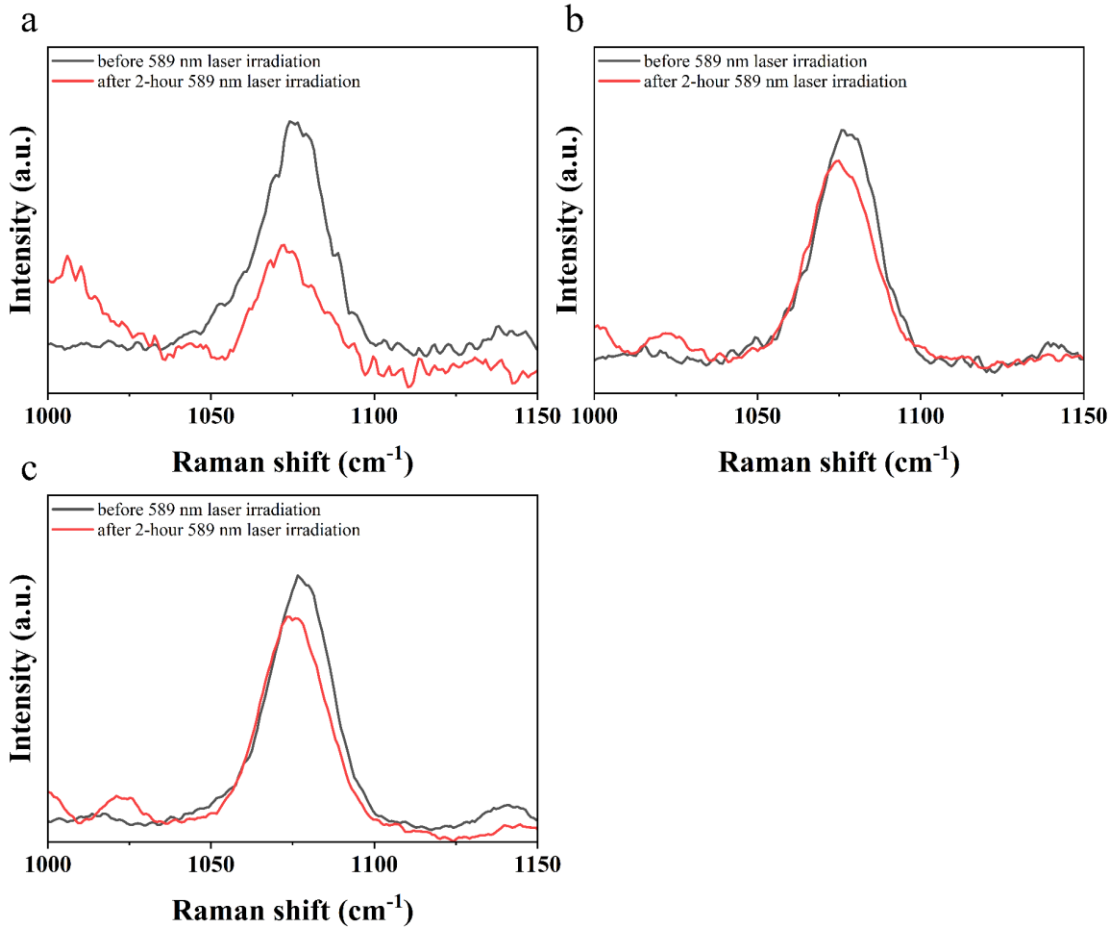

Fig. S6. (a-c) Raman peak at 1078 cm^{-1} of 4-MBA/AgNPs/C particle (from the corresponding panels of Fig. S5.a-S5.c) before and after 589 nm laser irradiation for 2 h.

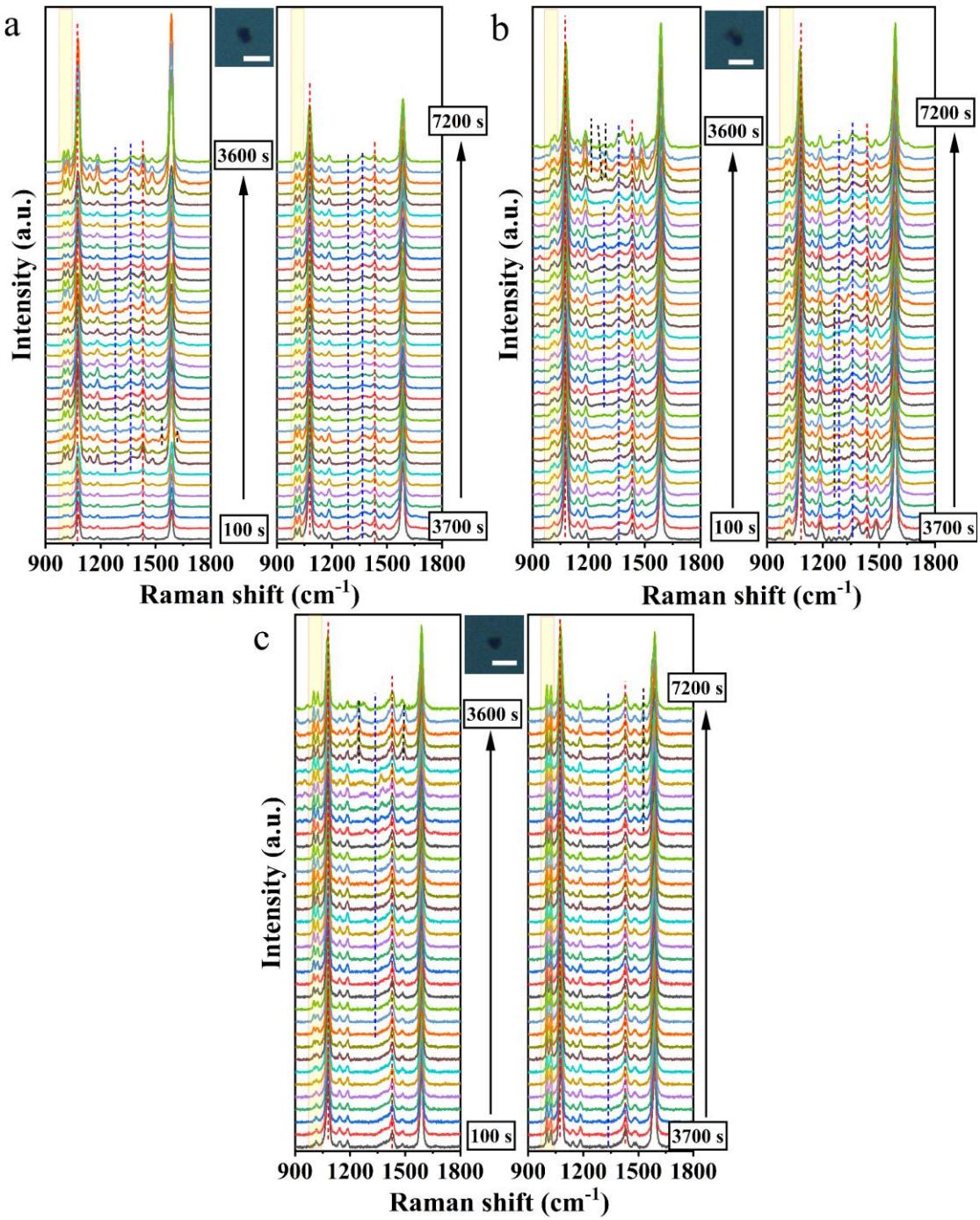

Fig. S7. (a-c) Temporal OT-SERS spectra and optical image of three 4-MBA/AgNPs/C particles under 671 nm laser irradiation. Scale bar: 10 μm.

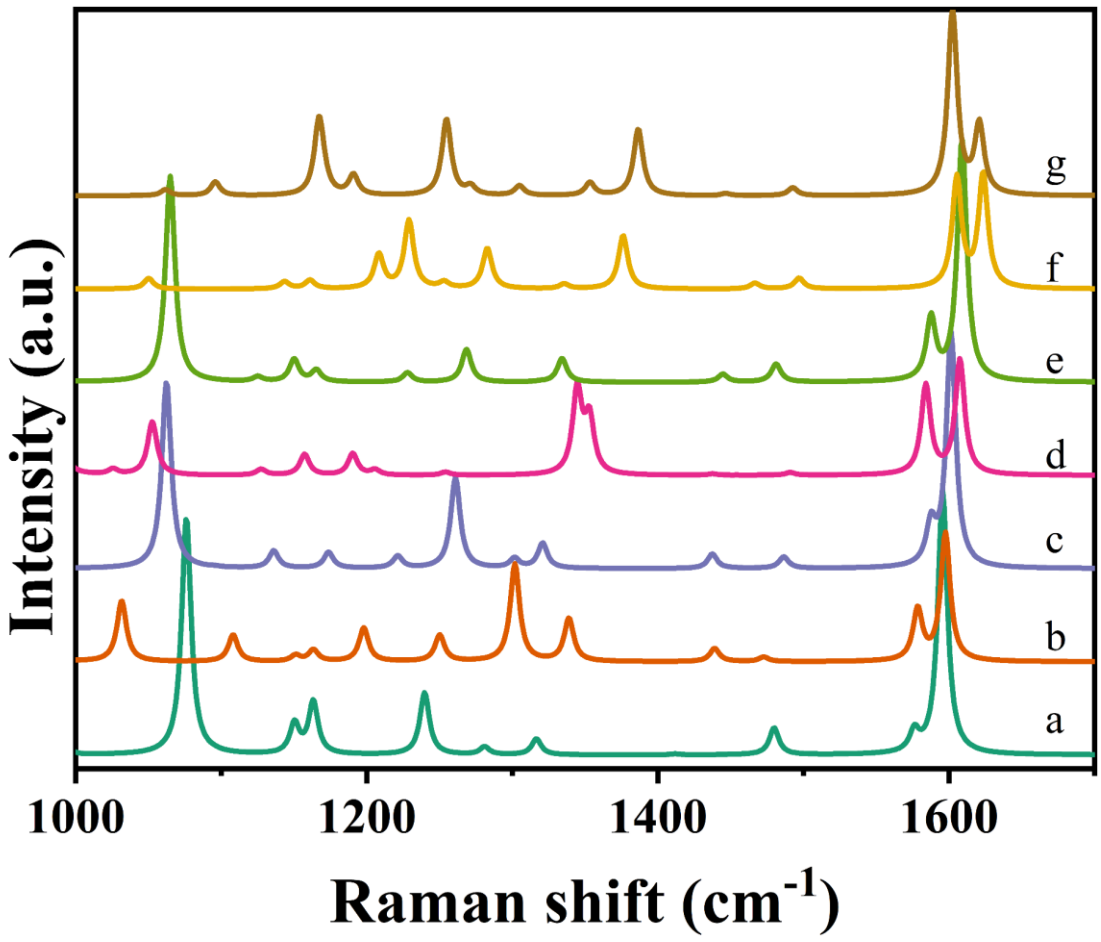

Fig. S8. Calculated Raman spectra of (a) 4-mercaptophenol, (b) 2,4-dihydroxybenzenethiol, (c) 3,4-dihydroxybenzenethiol, (d) 2,4,6-trihydroxybenzenethiol, (e) 3,4,5-trihydroxybenzenethiol, (f) 2,3,4,5-tetrahydroxybenzenethiol and (g) pentahydroxybenzenethiol.

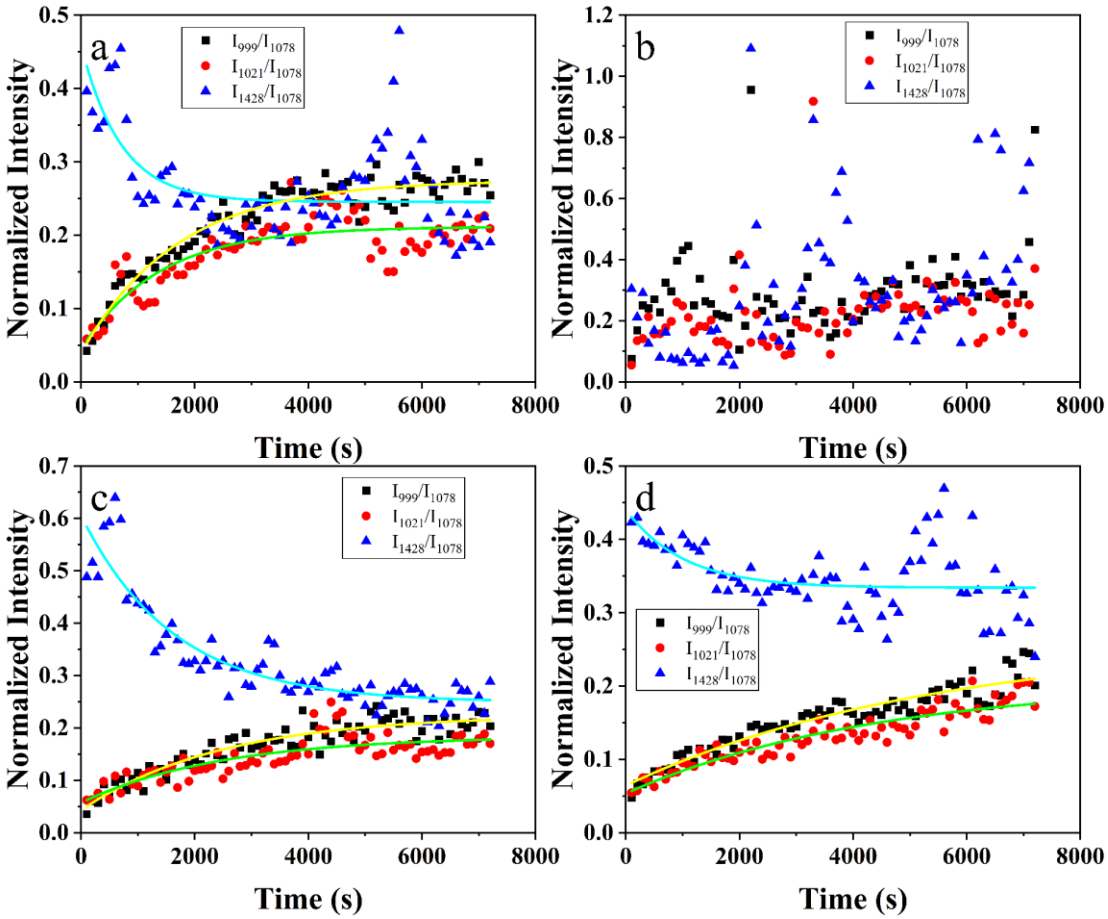

Fig. S9. (a-d) Variation trend of peak intensities at 999, 1021 and 1428 cm^{-1} of 4-MBA/AgNPs/C particle (from the corresponding panels of Fig. 5 and Fig. S5.a-S5.c) under 589 nm laser irradiation.

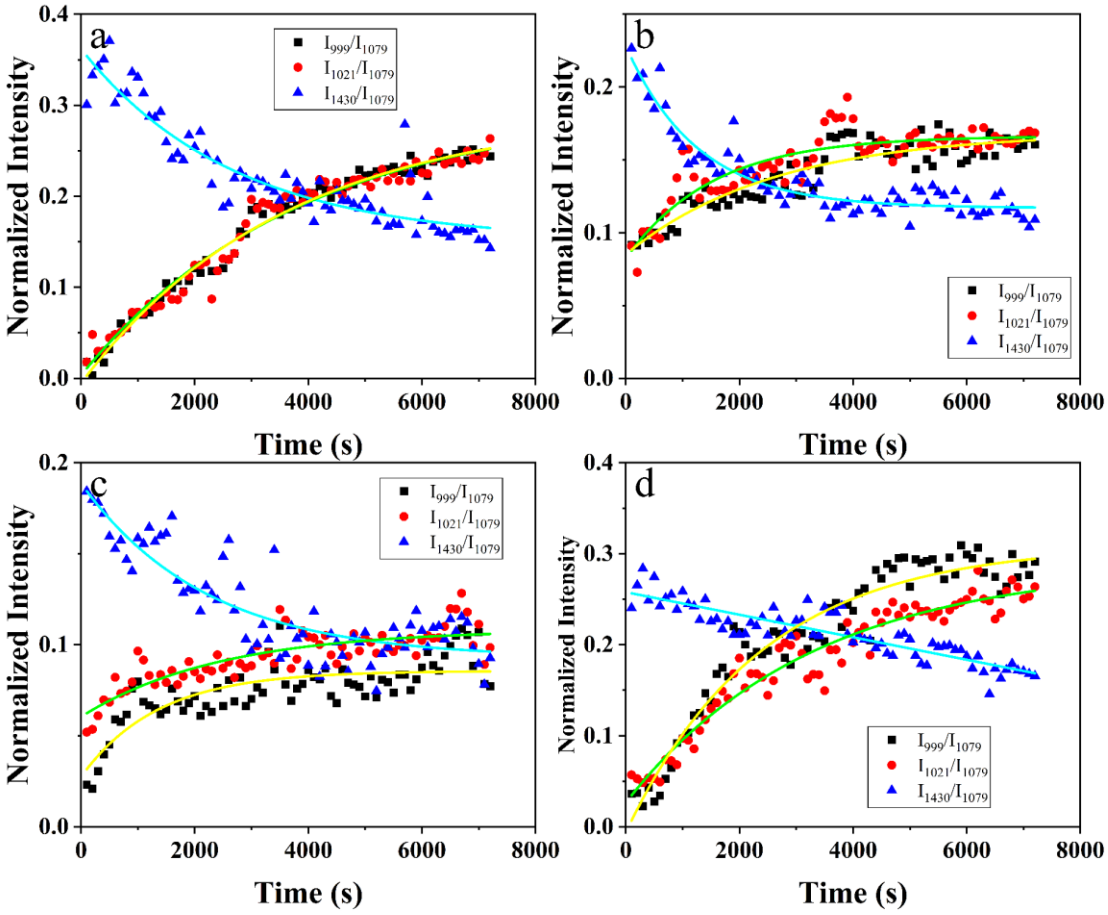

Fig. S10. (a-d) Variation trend of peak intensities at 999, 1021 and 1430 cm^{-1} of 4-MBA/AgNPs/C particle (from the corresponding panels of Fig. 7 and Fig. S7.a-S7.c) under 671 nm laser irradiation.